

RF Sheath-Enhanced Beryllium Sources at JET's ICRH Antennas

C C Klepper¹, P Jacquet², V Bobkov³, L Colas⁴, T M Biewer¹, D Borodin⁵, A Czarnecka⁶, C Giroud², E Lerche⁷, V Martin⁴, M-L Mayoral², F Rimini², G Sergienko⁵, D Van Eester⁷ and JET EFDA contributors*

JET-EFDA, Culham Science Centre, Abingdon, OX14 3DB, UK

¹Oak Ridge National Laboratory, Oak Ridge, TN 37831-6169, USA.

³Max-Planck-Institut für Plasmaphysik, EURATOM-Assoziation, Garching, Germany

⁵Assoc. EURATOM-FZJ, Trilateral Euregio Cluster, 52425 Jülich, Germany

* See the Appendix of F. Romanelli et al., Fusion Energy 2010 (Proc. 23rd Int. FEC Daejeon, 2010) IAEA, (2010)

²EURATOM/CCFE Fusion Assoc., Culham Science Centre, Oxon. OX14 3DB. UK.

⁴CEA, IRFM, F-13108 Saint Paul-Lez-Durance, France.

⁶Assoc. Euratom-IPPLM, Hery 23, 01-497 Warsaw, Poland

⁷Assoc. EURATOM-Belgian State, ERM-KMS, Brussels, Belgium

ABSTRACT

Local beryllium (Be) I and Be II line intensities were measured in the plasma-wall interaction region in the proximity of one ICRH antennas of JET. The immediate goal was to use these intensities as a measure of the formation of local RF sheath potentials, though rectification of RF electric fields in the plasma. Experiments, in which 3 antenna systems are modulated sequentially, have shown clear correlations between peaks in local Be I and Be II emission and the specific antenna that is active when these emission peaks occur. Furthermore, for the largest observed Be emission increase, magnetic field mapping indicates a direct connection between the observation location and the top corner region of the active antenna, which is consistent with computationally predicted poloidally-asymmetric electric field distributions. Experimental confirmation of computationally predicted sheath potential effects is an important part of the validation of antenna models needed to design antennas for next generation fusion energy devices, including ITER.

MOTIVATION

Using existing spectroscopic sightlines on ICRH Antenna structures to look for evidence of dc sheath formation, by looking for correlations between local Be line emission at PFCs and RF power of antenna(s) connected to these location.

RF Sheath Rectification Model [1]:

Parallel to similar study of W I on AUG all W antennas [2]

EXPERIMENTAL SETUP:

Existing sightlines of the JET CXRS diagnostic already terminated on antenna structures:

- Specifically the Octant 1 CXRS periscope has 12 chords, of which:
 - One passes near the "D-left" protection limiter and terminates on Strap D4 of Antenna D ← Refer to as "D4" chord (but source is likely from the limiter!)
 - One terminates on the "D-left" limiter ← Refer to as the "Limiter Chord"
- Both Be I 4572 Å (Singlet, 2s3d ¹D → 2s2p ¹P) and Be II 4673 Å (4f²F → 3d ²D) by the CXRS spectrometer but not in the same shot
- The non-localized C III 4650 Å was simultaneously detected, in both cases.

EXPERIMENTAL RESULTS

Experiments carried out in L-mode discharges using the JET A2 Antennas [3] in the ILW environment [4]

Most shots were designed to have all available antennas modulated sequentially.

- Antennas C and D were operated independently (all 4 straps functioning), while Antennas A&B were operated as a single antennas (2 straps from each)
- Edge q₉₅ was swept in some of these shots to change magnetic connections
- Substantial changes in Be I emission were observed, on the "D4" sightline, when Module C was active (Pulse 81173, Fig. 2).
- Similar response was seen with Be II emission (Pulse 81172, not shown).
- This effect was clearly q₉₅ dependent.

Clearly a Be source effect:

- Antenna-specific response of Be I and Be II hold even when the lines are divided by C III intensity to correct for local plasma parameters.

A SHEATH ENHANCED SPUTTERING?

Further analysis of pulses 81172/81173 showed:

- Clear differences in q₉₅ dependence in the emission from the antenna-side of the D-left limiter (Fig. 4). In particular:
 - C-antenna effect is high on both sides of the q₉₅ sweep
 - A&B-antenna effect increases monotonically with q₉₅
 - Global effects related to joint operation of the A-B pair?
 - OH (no-antenna) effect also increases monotonically with q₉₅ but not at same rate as A&B effect
- Clear link between the observation spot on D-left limiter and the top of Antenna C, as determined with EFIT-aided, magnetic field line tracing (Fig. 5)
 - This suggests that the enhanced, local Be source could be connected to the higher |E_{rf}| potentials predicted by antenna models for the poloidally extreme ends of the antennas.

EFFECT OF ANTENNA PHASING

- The fact that the observed, enhanced Be emission, in response to the activation of specific antennas is a result of rectified electric field formations at the magnetically connected PFC surfaces is further evidenced by a strong dependence observed on the phasing of the active antenna module (Fig. 6).

CORRELATION TO INFORMATION FROM CAMERA IMAGES

- At least one of the diagnostic imaging cameras was equipped with a Be II line filter; however, the settings were not optimized for antenna region light levels during diverted discharges.
- A color camera (KL12) used by the operations groups generated images that included the poloidal limiter viewed by the spectrometer sightlines (Fig. 7)

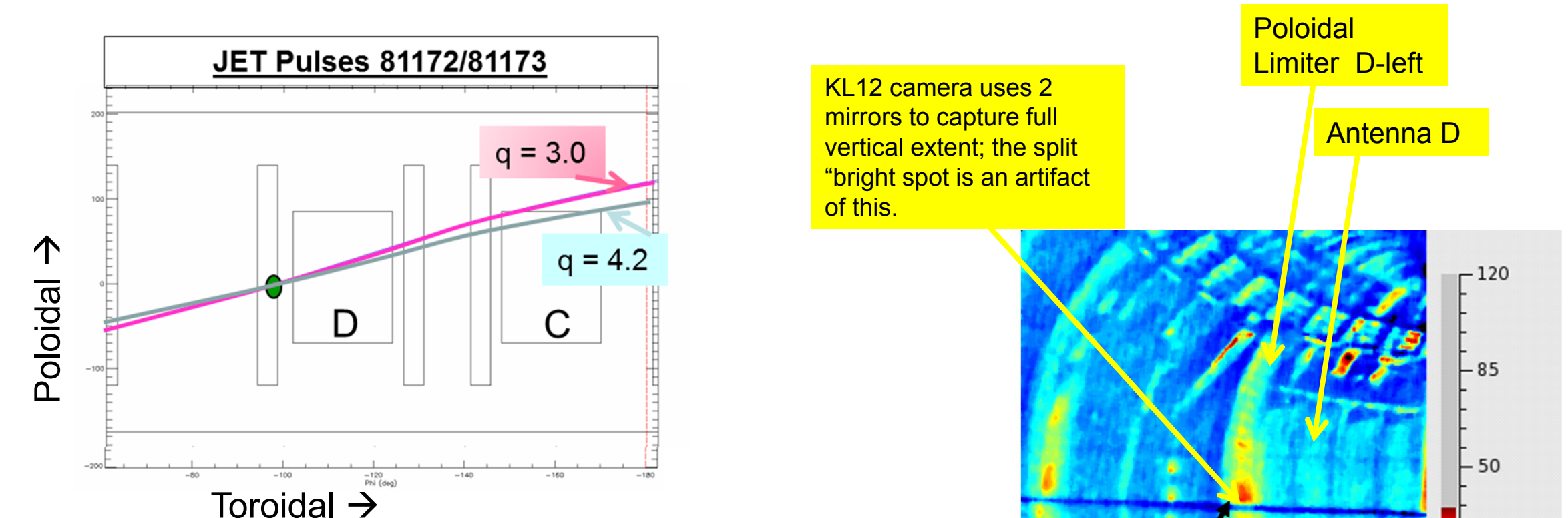


Figure 5: Magnetic field line tracing from antenna-side surface of D-left limiter to top region of antenna C.

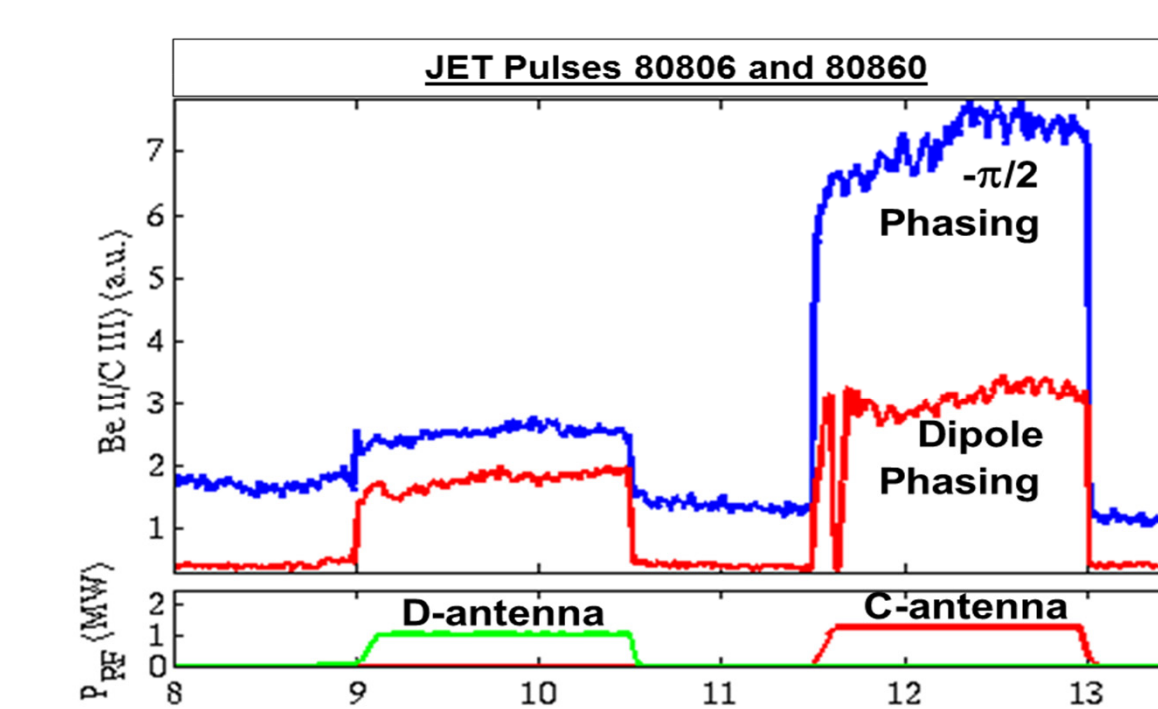


Figure 6: Comparison of the relative change in Be I/C III in two similar shots, primarily differing in the phasing of the antennas.

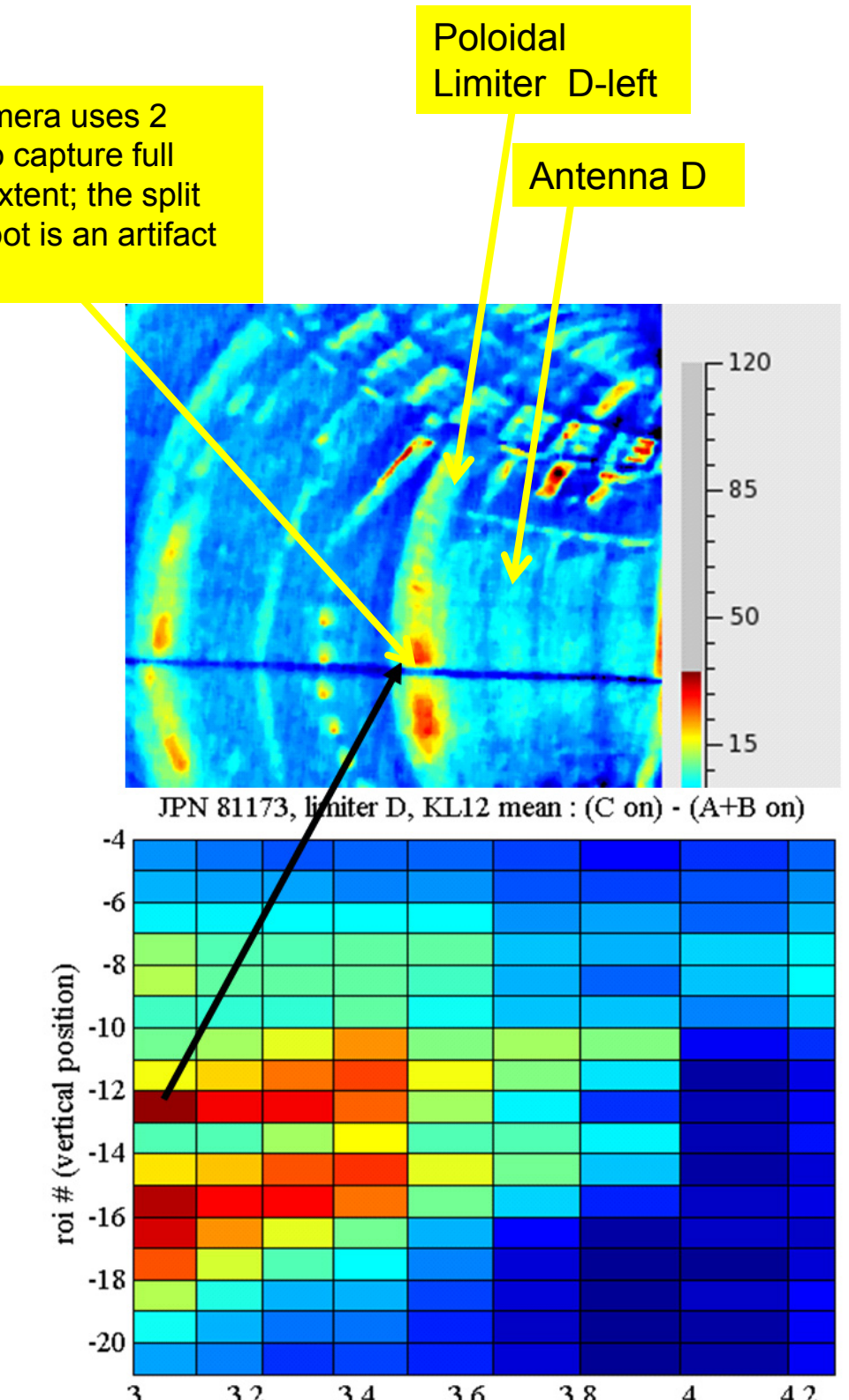


Figure 7: KL12 camera image capture at peak "C-ant ON" time and q-dependence of various poloidal points on the limiter. In bottom graph, the A&B-antenna average has been used as "background".

CONCLUSIONS and IMPLICATIONS FOR ITER

- Results indicate a clear correlation between localized, enhanced Be line emission at poloidal limiters and magnetic connections of these locations to active antennas
 - This constitutes a direct, experimental confirmation of ICRH induced, rectified rf-sheath potentials on magnetically connected PFCs.
 - ⇒ Important confirmation of effects predicted by ICRH antenna models.
- These results have been obtained in first ICRH experiments carried out in the JET ILW environment.
 - ⇒ Suggests that effects predicted by models developed in carbon and W environments will also apply in the Be/W environment of ITER

⇒ NEXT STEPS...

- Next step is to fold in JET ICRH Antenna-specific, numerical modeling, particularly to understand phasing-dependent effects and "global" effects from Antenna A&B
 - Also to confirm peaking of sheath potentials near the top of the antenna
- Improvement of camera imaging of ICRH antenna and protection limiters to get useful Be I or Be II line-filtered data.
- Connect the measurements to ADAS atomic physics models and Be erosion models (such as currently evolving versions of the ERO code [6], to get a preliminary evaluation of Be erosion in L-mode discharges
- Extend studies to H-mode. Be II line monitoring is compatible with CXRS on Be IV (5f - 6f' at 4659 Å).

ACKNOWLEDGEMENTS

This work was supported, in part, by EURATOM and carried out within the framework of the European Fusion Development Agreement. The views and opinions expressed herein do not necessarily reflect those of the European Commission. This work was also supported by the US DOE under Contract No. DE-AC05-00OR22725 with UT-Battelle, LLC.

REFERENCES

- [1] O.A. D'Ippolito, J.R. Myra, M. Bures et al., Plasma Physics and Controlled Fusion 33, No.6, 607 (1991)
- [2] V. Bobkov et al., Nucl. Fusion 50 (2010) 035004
- [3] A. Kaye, T. Brown, V. Bhatnagar, P. Crawley, et al., Fusion Engineering and Design 24, 1 (1994)
- [4] V. Philipps, Ph. Mertens, G.F. Matthews et al. Fusion Engineering and Design 85, 7-9, 1581 (2010)
- [5] L. Colas et al., Nucl. Fusion 45 (2005) 767-782
- [6] D. Borodin, A. Kirshner et al., Phys. Scr. T128 (2007) 127-132

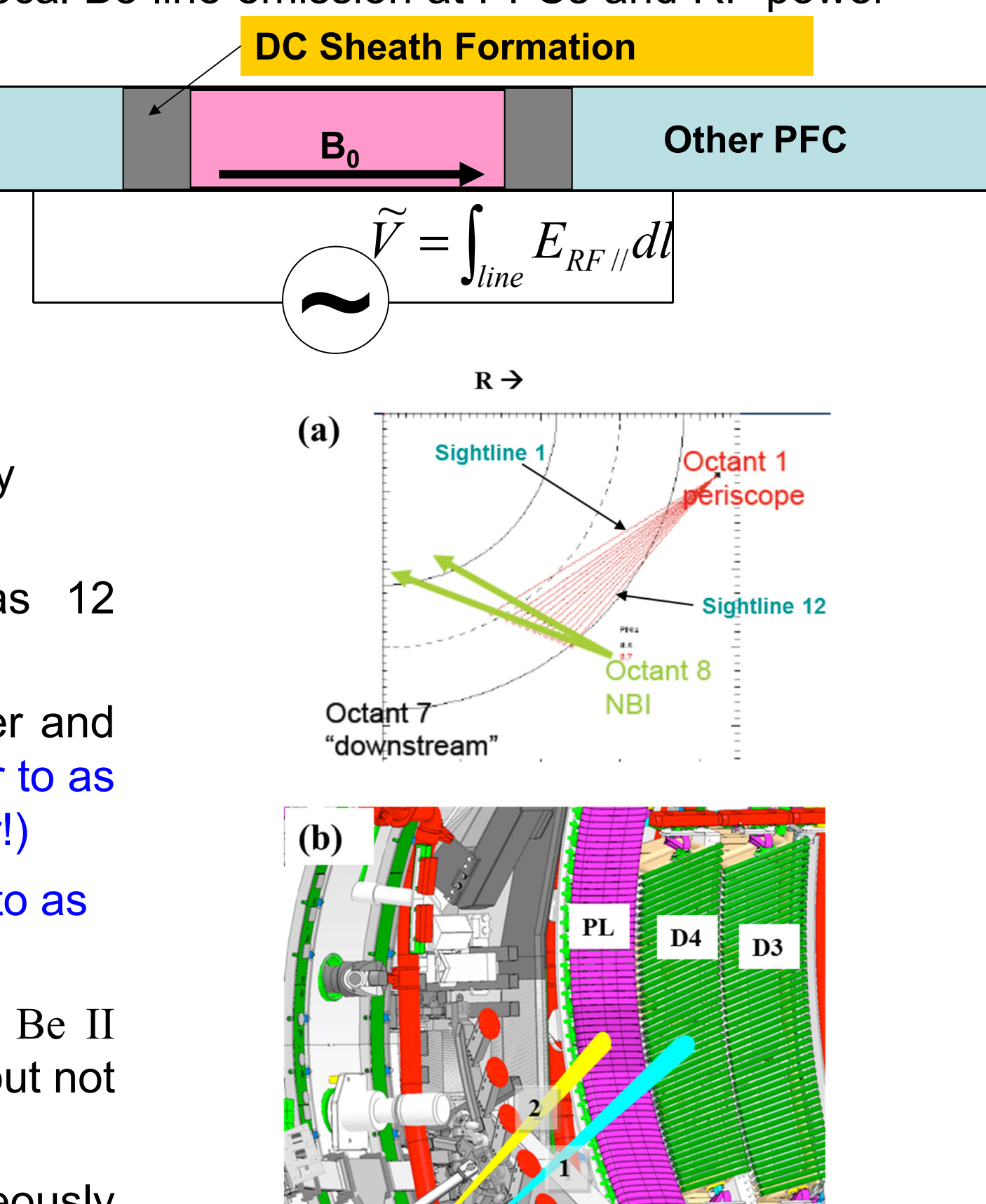


Figure 1: Illustration of spectroscopic sightlines accessing Antenna D structures.

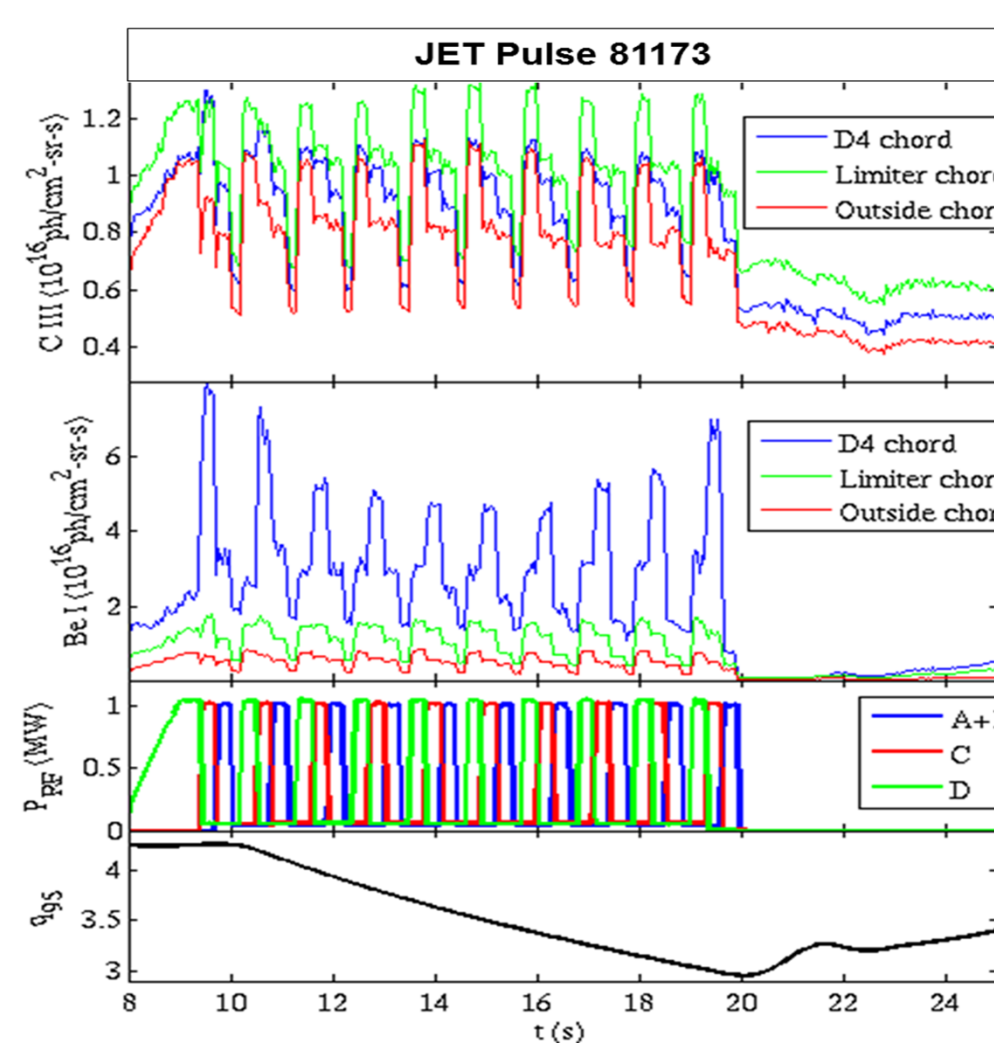


Figure 2: Separately plotted Be I and C III line intensities during q₉₅ sweep with antenna modulations

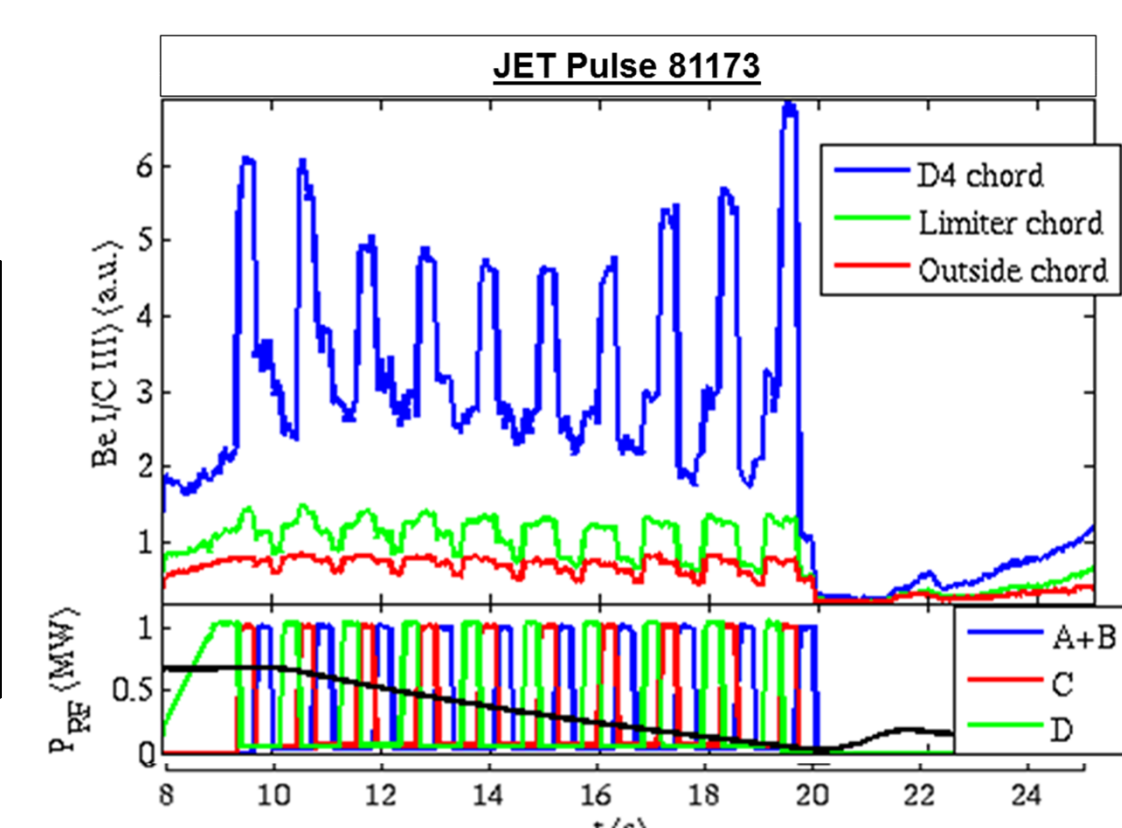


Figure 3: Ratio of Be I to C III line intensities during q₉₅ sweep with antenna modulations

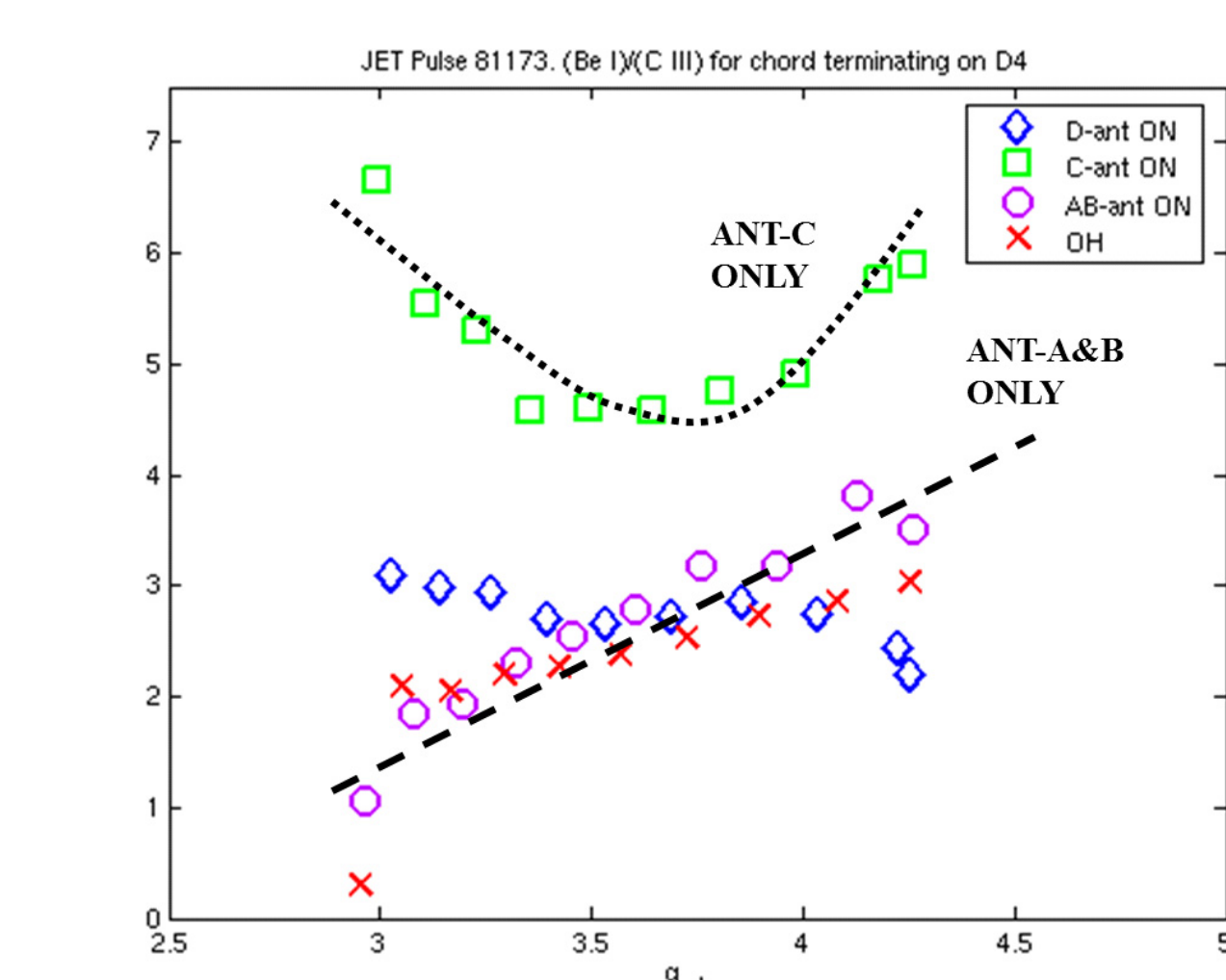


Figure 4: Ratio of Be I to C III averaged over the plateau of each of the antennas and for each cycle of the modulations (thus for each q₉₅ value). The dashed and dotted lines are just drawn to guide the eye.